Open Access Articles

Seasonal Cycle of Phytoplankton Community Composition in the Coastal Upwelling System Off Central Oregon in 2009

Seasonal Cycle of Phytoplankton Community Composition in the Coastal Upwelling System Off Central Oregon in 2009

Xiuning Du · William T. Peterson

Abstract Coastal upwelling in the northern California Current varies seasonally, with downwelling in winter and upwelling in summer, resulting in pronounced variability in hydrography, nutrients, phytoplankton biomass, and species composition. Winter was characterized by moderate concentrations of nitrate and silicate (averages of 10 and 18 μM, respectively) and low concentrations of chlorophyll *a* (Chl *a*). During the upwelling season, concentrations of the same nutrients ranged from near 0 μM to approximately 27 and 43 μM and Chl *a* $0.5<x<15$ μg L^{-1}. During autumn, upwelling weakened and nutrient concentrations were reduced, but large phytoplankton blooms continued to occur. Variations in hydrography, nutrients, and phytoplankton also occurred within the upwelling season due to alternation of the winds between northerly (active upwelling) and southerly (relaxation of upwelling), on a 5- to 10-day time scale. Eleven blooms were observed, most of which occurred near the end of active upwelling events and during relaxation of upwelling. Nonmetric multidimensional scaling ordination of species composition of the microplankton revealed four distinct communities: a winter community, early upwelling and late upwelling season communities, and an autumn community. Diatoms (*Asterionellopsis glacialis*, *Eucampia zodiacus*, and several *Chaetoceros*, *Thalassiosira*, and *Pseudo-nitzschia* species) dominated early in the upwelling season, averaging 80 % of the phytoplankton biomass, and dinoflagellates dominated near the end of the upwelling season, averaging 68 % of the phytoplankton biomass. Dinoflagellates formed two monospecific blooms—*Prorocentrum gracile* in late summer and *Akashiwo sanguinea* in autumn. Changes in community composition were correlated with bottom temperature and salinity (representing seasonal variability) and sea surface salinity (representing within-season event-scale variability in upwelling).

X. Du
College of Environmental Science and Engineering,
Ocean University of China,
Qingdao, Shandong 266100, China

X. Du
Cooperative Institute for Marine Resource Studies,
Hatfield Marine Science Center,
Newport, OR 97365, USA

X. Du (✉)
East China Sea Fisheries Research Institute,
Chinese Academy of Fishery Sciences,
Shanghai 200090, China
e-mail: xiuningdu@gmail.com

W. T. Peterson
NOAA Fisheries, Northwest Fisheries Science Center,
Hatfield Marine Science Center,
Newport, OR 97365, USA

Introduction

Coastal waters of the northern California Current are characterized by pronounced seasonal cycles in circulation patterns, temperature, and salinity, driven largely by large-scale wind fields over the northeast Pacific Ocean and local precipitation and runoff (Huyer 1977). Winter is the downwelling season resulting from strong southwesterly winds and is characterized by onshore and northward transport of warm low salinity water by way of the Davidson Current. These conditions persist generally from November through February or March. During summer, winds are northerly to northwesterly which cause upwelling at the coast and southward transport of cold high salinity water that has upwelled from depths of ~150 m from offshore continental slope regions (Hickey 1989). April/

May and September/October are months of transition and are often characterized by winds that alternate between southerly and northerly. Seasonal variations in the cycle of coastal upwelling give rise to large and well-described seasonal differences in nutrient and chlorophyll concentrations (Chavez et al. 1991; Henson and Thomas 2007; Kudela et al. 2008; Thomas et al. 2009; Tweddle et al. 2010; Yoo et al. 2008), copepod abundance and species composition (Peterson and Miller 1977), copepod community structure (Peterson and Keister 2003), as well as ichthyoplankton abundance and species composition (Auth 2011).

Significant variations in temperature, salinity, nutrients, and plankton also occur within the upwelling season as a result of event-scale variations in the winds which alternate between northerly and southerly on a 5- to 10-day time scale. Northerly winds drive surface waters offshore, and these are replaced by cold nutrient-enriched water which rise up to the sea surface nearshore; however, mixing rates can be too high to permit the development of phytoplankton blooms at such times; relaxations of the winds and/or southerly winds return surface water shoreward, leading to a stratified water column and large phytoplankton blooms. It is this alternation of the winds and offshore–onshore transport of surface waters that gives the coastal upwelling system of the northern California Current its extraordinarily high productivity (Hickey and Banas 2008). Blooms typically exceed 10–20 μg Chl a L^{-1} during summer months (Feinberg and Peterson 2003).

Although seasonal cycles of nutrients and chlorophyll in the northern California Current have been well characterized, studies on phytoplankton species composition and community structure in the coastal upwelling domain of the west coast of North America are limited to a handful of studies that have focused exclusively on dynamics only during the summer upwelling seasons. Hood et al. (1990) and Chavez et al. (1991) observed strong connections between diatom-dominated phytoplankton communities with cold, nutrient-enriched coastal water off northern California. Lassiter et al. (2006) reported that diatom communities dominated the phytoplankton biomass during summers of 2000, 2001, and 2002 near Pr. Reyes. Further north, Frame and Lessard (2009) were the first to consider the community of phytoplankton species in the continental shelf waters off Washington and northern Oregon, in work completed during the summers of 2004–2006. Two other local studies include phytoplankton species composition in enclosed bays: Dabob Bay, WA (Puget Sound) in winter/spring (Horner et al. 2005) and Willapa Bay, WA (Newton and Horner 2003). In the southern California Current, Venrick (2012) described cross-shelf differences in phytoplankton assemblages, but she has also provided some information on seasonal cycles, based on samples collected quarterly.

Seasonal cycles of phytoplankton biomass and species composition have been described for other upwelling ecosystems,

but again, there are very few published studies (Pitcher et al. 2010). In the Humboldt Current off central Chile, diatoms, such as *Chaetoceros*, *Thalassiosira*, and *Asterionellopsis*, were the largest components in terms of biomass and made important numerical contributions during the upwelling season from September 2003 to August 2004 (Anabalón et al. 2007). A 4-year study (weekly cruises from July 2001 to May 2005) in Lisbon Bay, Portugal (Silva et al. 2009) revealed that diatoms (mainly in the genera of *Chaetoceros*, *Thalassiosira*, and *Pseudo-nitzschia*) dominated the spring–summer upwelling season. Coccolithophores were the second most abundant category, dominating the community in response to the event-scale alteration from upwelling to downwelling and during the post-upwelling autumn and winter seasons.

The present study aims to shed light on the seasonality of species composition, community structure, and biomass of phytoplankton in the northern California Current from sampling carried out along the central Oregon Coast. The relationships between seasonality of circulation, upwelling, copepods, and larval fish are strong at this location (Auth 2011; Hooff and Peterson 2006; Peterson et al. 2002; Peterson and Keister 2003; Peterson and Miller 1977), but the concurrent response of phytoplankton community composition has not been systematically evaluated. Here, we add, for the first time, data on seasonal variations in phytoplankton species composition and abundance from samples taken during the year 2009. To the best of our knowledge, this manuscript contributes the first data from the northern California Current upwelling ecosystem that describes year-round variations in phytoplankton community composition. We include a discussion of high-frequency variations in hydrography, nutrients, chlorophyll, and phytoplankton community composition resulting from event-scale variations (5- to 10-day variability) in upwelling. This study is part of a larger study of harmful algae in coastal waters off Oregon called project MOCHA (Monitoring Oregon's Coastal Harmful Algae).

Methods

Data Collection

Hydrographic, nutrient, and phytoplankton data were collected biweekly from the Newport Hydrographic (NH) Line at a single station (referred to as NH05, 44.65° N, 124.18° W), 9 km from the shore off central Oregon, USA, in 60 m water depth. Sampling dates are listed in Table 1. Charts showing station location have already been published (Du et al. 2011; Feinberg et al. 2010; Hooff and Peterson 2006). This station is located at/near the center of the most active upwelling zone; therefore, strong variations are seen in the transport, hydrography, nutrients, chlorophyll, and abundance of planktonic species.

Table 1 Sampling dates at station NH05 on the NH Line in 2009, daily SST anomaly at NOAA Buoy 46050, status of upwelling and phytoplankton bloom on each sampling date, phytoplankton biomass (Chl a concentration and carbon), nitrate concentration, percentage of Chl a <5 μm, SST and SSS observed at NH05, "cluster" column corresponds with clusters from "CLUSTER" and "NMDS" community structure analysis

Dates (month/day)	SST anomaly	Status of upwelling and phytoplankton bloom	Total C (μg C L^{-1})	Total Chl a (μg L^{-1})	NO$_3$ (μM)	SiO$_4$ (μM)	PO$_4$ (μM)	Chl a <5 μm (%)	SST (°C)	SSS	Cluster
1/14	−0.93	Winter	–	0.9	13.2	24.9	1.2	72.2	9.2	30.7	–
1/23	−0.91	Winter	–	2.2	10.3	18.3	1.1	78.3	8.8	31.9	–
2/4	−1.03	Winter	1.0	0.8	9.1	18.4	0.9	62.7	8.4	31.0	A
2/17	−1	Winter	8.0	1.7	10.7	15.1	1.1	41.1	8.7	32.4	A
3/6	−0.49	Winter	–	0.8	8.5	14.6	1.0	59.3	9.7	32.2	–
3/24	−0.57	Upwelling season begins	2.7	1.8	7.4	14.0	0.9	71.1	9.5	32.2	A
4/4	−1.3	Large bloom; end of upwelling event "a"	286.6	9.3	0.6	4.3	0.2	91.6	9.1	30.9	B
4/7	−1.03	large bloom; beginning of relaxation "1"	–	11.1	4.1	8.7	–	32.5	–	–	–
4/23	−1.69	Pre-bloom; upwelling-limited growth	8.0	0.6	15.9	23.2	1.5	5.8	8.8	32.7	A
5/7	−1.48	Small bloom during relaxation "2"	246.7	4.4	0.1	1.2	0.1	61.4	11.2	31.2	B
5/16	−0.97	Post-bloom during relaxation "2"	0.7	1.4	0.1	0.8	0.2	72.6	11.7	31.2	A
5/26	−1.81	Bloom initiated during upwelling event "c"	90.0	5.0	18.6	34.0	1.8	46.3	10.9	33.2	B
6/2	0.18	Large bloom during relaxation "3"	479.8	15.1	0.4	19.1	0.1	72.6	11.5	33.2	B
6/14	−0.07	Post-bloom; nutrient-limited growth	22.8	0.5	1.3	1.4	0.2	4.1	12.7	32.1	D
6/30	−4.45	Bloom initiated (event "d"); upwelling-limited growth	–	0.97	26.6	43.1	2.2	–	7.95	33.6	–
7/8	−0.21	Large bloom; end of upwelling event "d"	460.4	9.1	0.2	3.4	0.2	70.5	11.3	33.2	B
7/12	1.19	Post-bloom during relaxation "4"	–	2.8	0.1	0.9	0.2	40.1	12.9	32.7	–
7/23	−2.23	Large bloom; during upwelling event "e"	485.5	13.3	16.8	29.7	1.5	57.0	9.2	33.6	B
7/28	−0.49	Large bloom; during but end of upwelling event "e"	406.1	14.5	14.1	31.3	1.5	50.3	10.4	33.6	B
8/14	2.8	Post-bloom; nutrient-limited during relaxation "5"	–	1.1	–	0.5	0.2	44.7	15.5	32.8	–
8/27	0.27	Large bloom; nutrient-limited at end of event "f"	952.2	10.7	1.9	7.9	0.4	58.9	12.0	32.9	C
9/10	1.39	Post-bloom; nutrient-limited, mid-relaxation "6"	25.4	3.2	0.4	1.0	0.3	34.2	14.5	32.7	C
9/22	3.45	Large bloom; end of relaxation "6"	965.2	15.6	0.2	1.0	0.1	53.2	16.7	32.6	C
9/29	−0.8	Pre-bloom; strong upwelling-limited growth	–	0.81	15.7	22.0	1.5	–	9.37	33.3	–
10/5	0.65	Large bloom; end of upwelling event "g"	1,907.8	11.6	0.6	2.0	0.3	65.6	11.7	32.9	B
10/19	1.84	Large bloom; post upwelling season; relaxation "7"	137.5	20.9	1.3	8.4	0.6	64.0	12.7	32.6	D
11/4	0.51	Large bloom; post upwelling season; relaxation "7"	189.5	20.7	0.8	10.1	0.7	86.2	12.2	32.1	D
11/10	1	Winter	72.3	2.1	2.8	6.8	0.6	40.7	11.9	32.4	D
12/1	−0.02	Winter	8.6	0.6	7.2	15.5	0.9	37.2	10.7	31.6	A
12/23	−0.83	Winter	–	1.1	10.4	18.2	1.0	35.0	9.53	31.6	–

A data are not available because samples were not taken

On each cruise, vertical profiles of temperature and salinity were made with a Seabird SBE 19 CTD. Water samples were taken from the sea surface for later analysis of nutrients (phosphate, silicate, nitrate, and ammonium), chlorophyll *a* (Chl *a*; total and >5 μm size fraction), and phytoplankton species. Total and >5 μm Chl *a* fraction subsamples (each of 100 ml with two replicates) were filtered through GF/F filters and 5 μm polycarbonate filters, respectively, extracted in 90 % acetone for 24 h in the dark, and then were analyzed on a Turner 10-AU fluorometer. The concentration of total Chl *a* was calculated following Strickland and Parsons (1972); the concentration of Chl *a* <5 μm size fraction was calculated based on the total and >5 Chl *a* fractions. Nutrients were processed by J. Jennings (School of Earth, Ocean and Atmospheric, Oregon State University) using a Technicon Autoanalyzer, following standard protocols.

Phytoplankton samples (150 ml of seawater) were fixed with formalin (final concentration, 2 %) and processed in the laboratory as detailed in the study of Du et al. (2011). Briefly, a subsample was taken from the original sample bottle and poured into a 50-ml Falcon culture flask, and then the flask was set on its wide side on the stage of an inverted light microscope (Leica DM IRB) and allowed to settle for at least 24 h prior to counting. Our efforts were focused mostly on the diatoms and dinoflagellates which were counted at ×200 or ×400 magnification. Identifications were made using primarily the method of Horner (2002). Nanoflagellates and picoplankton were not enumerated in part due to the use of formalin as a preservative and also due to difficulties in identifying individuals to species—however, their contribution to total biomass is approximated by the data on the concentration of Chl *a* in the <5 μm size fraction. Abundances of diatoms, dinoflagellates, and other taxa were estimated by counting several transects that spanned the width of the culture flask. The number of transects counted depended on cell abundance. Phytoplankton cell volume was calculated based on simple geometric formulas by measuring appropriate dimensions of 20–30 individuals of each species in each sample. The microscopic method of estimating cell volume limits measurements to one or two dimensions depending on cell views, so we determined some cell volumes from published literatures (Menden-Deuer and Lessard 2000; Menden-Deuer et al. 2001; Olson and Lessard 2008). Cell carbon (in micrograms C per liter) was converted from cell volumes according to Menden-Deuer and Lessard (2000).

The Bakun Upwelling Index (BUI; http://www.pfeg.noaa.gov/products/PFEL) indicates the strength and variations of the coastal upwelling along the latitude of 45° N. The cumulative upwelling index (CUI) was used to define the upwelling season and was calculated by adding the value of the BUI on 1 day to that of the next day and so on, beginning with 1 January through 31 December. Hourly sea surface temperature (SST) collected at the NOAA Buoy 46050 (44.64° N, 124.50° W) was used to compute daily and monthly averages of SST

(http://seaboard.ndbc.noaa.gov). Climatological averages are based on the entire 18-year record, 1991–2008.

Phytoplankton Community Structure Analysis

All multivariate analyses were run on PRIMER-E version 6.0 (Clarke and Gorley 2006). Hierarchical cluster analysis (CLUSTER) and nonmetric multidimensional scaling (NMDS) were performed on the matrix of "species carbon biomass" × "sample date" to examine similarities in phytoplankton community composition among sampling dates; Bray–Curtis similarity and group average linkage options were used. Phytoplankton species biomass were $\log(x+1)$ transformed to achieve normality. In the NMDS ordination plot, sampling dates are represented as points in a two-dimensional ordination; points that are close together indicate samples similar in community composition and vice versa; "stress" indicates how faithfully the reduction from a high-dimensional relationship is represented by a low-dimensional ordination. Similarity Percentage (SIMPER) analysis was implemented to determine which species contribute the most to each cluster. The linking of phytoplankton assemblages to environmental factors was examined by BEST/BIO-EVN analysis. The combinations with the highest Spearman's rank correlation coefficient (ρ) match phytoplankton community structure the best. Linear regression analysis was used to test correlations (significance level: $p=0.05$) between environmental variables and x-axis scores derived from NMDS ordination (expressing species community changes) by using the SigmaPlot v.10 software.

Results

Coastal Upwelling

Monthly SST anomalies from the 18-year climatology indicate that the coastal ocean in 2009 was cooler than normal from January to July (blue bars) and in December, but warmer than average (red bars) from August to November (Fig. 1). The CUI plot (Fig. 2) shows that the upwelling season was initiated approximately on 23 March and continued until 12 October. Moreover, upwelling was not a continuous process, rather "active" upwelling events alternated with "relaxation" events (associated with reversals in the winds) and these occurred frequently in May, mid-June, and mid-July. A total of seven active upwelling events were observed (as indicated by the lowercase letters: "a" through "g" in Fig. 2 which mark periods when the slopes in the CUI plot were positive); these were interspersed with six "relaxation" or "downwelling" events (the numbers "1" through "6" in Fig. 2 associated with plateaus in the CUI plot). The upwelling season ended on 12 October, after which seasonal downwelling was initiated (the number "7" in Fig. 2). Further, the upwelling season was

strong early in the season (May through July) then became relatively weak throughout much of August and September: between 1 May and 31 July, the cumulative total upwelling averaged ~42 units day^{-1}, whereas from 1 August until the end of the season on 12 October, upwelling averaged ~17 units day^{-1}.

Seasonal Variations in Environmental Factors

SSTs were low during January to March (8.4–9.7 °C) but increased above 10 °C from May to July (Table 1). Two higher values were observed, on June 14 (12.7 °C) and July 12 (12.9 °C) during the third and fourth relaxation events (indicated by the number "3" and "4" in Fig. 2). The warmest SSTs appeared in September (maximum of 16.7 °C on 22 September, an anomaly of 3.5 °C greater than the climatology for that date; Table 1). SST decreased to an average of 12.3 °C in autumn due to seasonal cooling. Sea surface salinity (SSS) ranged from 30 to 32 in winter and spring and was relatively low due to precipitation and runoff from local rivers. During the upwelling season, values in excess of 33 indicate active upwelling (for example, as on 26 May and 2 June) and values slightly less indicate a relaxation of upwelling (as on 14 June and 12 July). The highest SSS (~33.6) was found on 30 June, 23 July, and 28 July during the strong upwelling events (letters "d" and "e" in Fig. 2). SSS remained at or above 32.6 throughout the late summer and early autumn (through the 19 October cruise), after which seasonal downwelling and lower salinities were observed.

Nutrient concentrations during the winter downwelling season averaged ~10 and 18 μM for nitrate and silicate concentrations, respectively, but were highly variable during the summer upwelling season (Fig. 2). Values of NO_3 and $Si(OH)_4$ covaried with six peaks of 15.9, 18.6, 26.2, 16.8, 14.1, and 15.7 μM for NO_3 and 23.2, 34.0, 43.1, 29.7, 31.3, and 22.0 μM for $Si(OH)_4$ on cruises on 23 April, 26 May, 30 June,

Fig. 2 Cumulative daily upwelling index at 45° N, 125° W and nutrient concentrations. The upwelling season extended from 23 March to 12 October in 2009. *Lowercase letters* ("a" through "g") adjacent to the positive slopes of the CUI indicate the seven active upwelling events; *numbers* ("1" through "6") adjacent to the plateaus in the CUI indicate the six downwelling events. The end of the upwelling season and the beginning of the seasonal downwelling is indicated by "7." The *vertical lines* associated with peaks in nutrients were drawn to aid in illustrating that peaks in nutrients are associated with active upwelling events "b" through "g"; very low values are associated with relaxation events "2" through "6"

23 and 28 July, and 29 September, respectively—each of these peaks was observed during an active upwelling event (events "b," "c," "d," "e," and "g" in Fig. 2). Very low values of NO_3 and $Si(OH)_4$ were observed during downwelling (events "2" through "6"). After the end of the upwelling season (from mid-October through mid-November), silicate concentrations increased (up to 10 μM) but nitrate concentrations remained low (<2.8 μM). Relatively high PO_4 concentrations (1.5–2.2 μM) were found during the same six upwelling events as NO_3 and $Si(OH)_4$ and lower concentrations during the downwelling events (Table 1). NH_4 concentrations (not shown) were always <0.4 μM (with one exception on 12 July) throughout the summer upwelling season and autumn downwelling period.

Seasonal Variations in Chlorophyll Concentration, Phytoplankton Biomass, and Species Composition

A total of 11 phytoplankton blooms were observed during this study, arbitrarily defined as occurring on dates when total Chl a concentration exceeded 4 μg L^{-1}. Nine occurred during the upwelling season (24 March through 10 October). Of these nine blooms, most occurred towards *the latter stages of* or *near the end of* upwelling events (Table 1; Fig. 3), when SST values ranged from 9.1 to 12.0 °C. Two of the nine blooms coincided with peaks in nitrate concentration averaging 16.5 μM (26 May and 23 and 28 July), but for five of the nine, nitrate concentrations were very low (4 April, 7 May, 2 June, 8 July, and 5 October), averaging 0.38 μM. These blooms were caused by diatoms (based on the microscopic observations), as will be shown in the succeeding paragraphs. Of the other two blooms observed
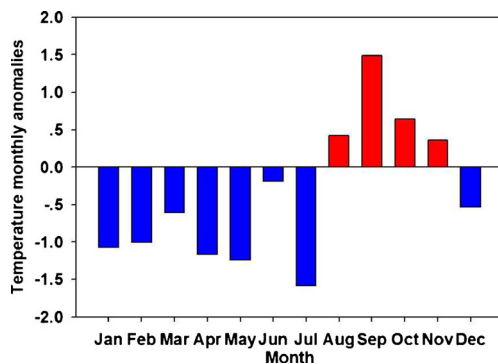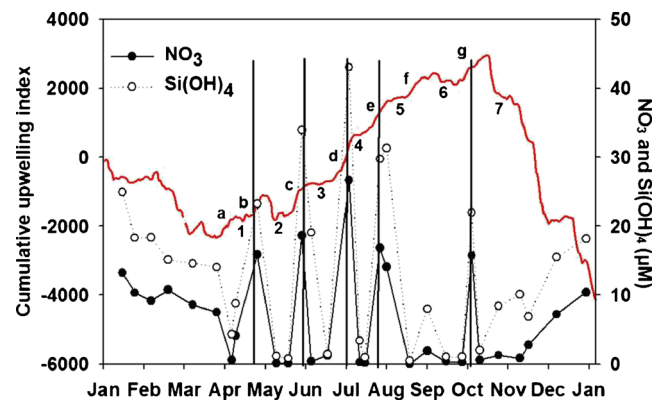
Fig. 1 Monthly anomalies of SST based on hourly SST from NOAA Buoy 46050, located 22 mi offshore, Newport, OR, in 2009. The *red bars* (from August to November) indicate warm ocean periods and the *blue bars* (January to July, December) indicate cold ocean periods

during the upwelling season, one was on 27 August when nitrate concentration was relatively low (1.9 μM) and the other was on 22 September. This late September bloom was unusual in that it had the third highest Chl *a* value (15.6 μg L^{-1}), among the lowest nitrate (0.2 μM), and the highest SST (16.7 °C) observed during the study and was the only bloom observed *very late in a relaxation event*. As will be shown in the succeeding paragraphs, both the 27 August and 22 September blooms were composed chiefly of dinoflagellates.

Chl *a* was low when nitrate was very high on four dates (averages of 1.1 μg L^{-1} Chl *a* and 16.4 μM nitrate)—these dates were at the *beginning* of upwelling events (24 March, 23 April, 30 June, and 29 September) when SST averaged 8.9 °C. On four other dates, both Chl *a* and nitrate were very low (1.9 μg L^{-1} and 0.45 μM)—these dates were all "post-bloom," during relaxation of upwelling (16 May, 14 June, 12 July, and 10 September). Two blooms occurred outside of the upwelling season on 19 October and 4 November. Both had the highest Chl *a* values (average of 20.8 μg L^{-1}) and low nitrate (1.05 μM), and both were associated with dinoflagellates.

Seasonal variations in phytoplankton biomass (in carbon unit) and species composition also reflect the seasonality of upwelling, light availability, SST, and nutrient concentrations. Phytoplankton carbon biomass in winter ranged from 1.0 to 8.6 μg C L^{-1} (Table 1; Fig. 4), and total Chl *a* concentration was relatively low, ranging from 0.6 to 2.2 μg L^{-1} (Table 1). Diatoms and dinoflagellates averaged 58.8 and 16.1 % of total carbon biomass, respectively. The dominant species enumerated during winter belonged mainly to diatoms: *Chaetoceros* spp. (*Chaetoceros lorenzianus* and *Chaetoceros teres*), *Thalassiosira* spp. (*Thalassiosira pacifica/aestivalis* and *Thalassiosira nordenskioeldii*), and some discoid diatoms.

In spring and early summer, phytoplankton biomass increased greatly but with large variations (range of 0.7 to
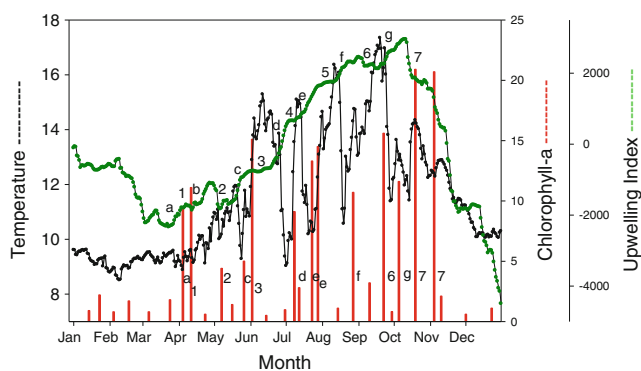

Fig. 3 Relationships between chlorophyll concentration (*red bars*), daily SST at NOAA Buoy 46050 (*black line*), and the cumulative daily upwelling index (CUI). The *letters* and *numbers* associated with the CUI plot are the same as in Fig. 2. The *letters* and *numbers* in the lower part of the graph adjacent to the chlorophyll bars indicate which "events" correspond with chlorophyll *a* values
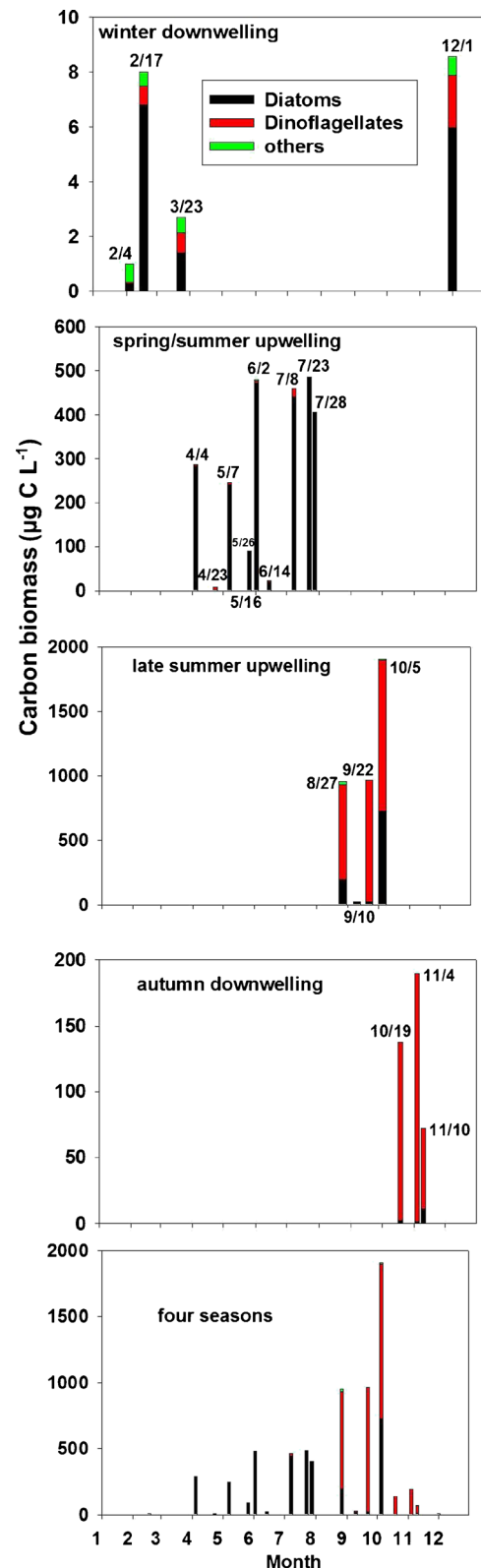

Fig. 4 Seasonal variations in carbon biomass of diatoms, dinoflagellates, and other species (cryptophytes, euglenophytes, silicoflagellates, and unknown flagellates) in 2009. Note the differences in scales on each graph. Sampling dates are labeled on the plots. The *last panel* shows the comparison among the four seasons, using the same scale on the *y*-axis

485.5 μg C L^{-1}). Large blooms were observed on 4 and 7 April (286.7 μg C L^{-1}), 7 May (246.7 μg C L^{-1}), 2 June (479.9 μg C L^{-1}), and in July (400–500 μg C L^{-1}) (Table 1; Fig. 4). Diatoms averaged ~80 % of the total phytoplankton biomass with high variability (27.4–99.7 %) and dinoflagellates averaged ~15 % of the total biomass. The proportion of Chl *a* in the <5 μm size fraction was high (40.1–91.6 %) with only two observations below 10 % on 23 April and 14 June; however, on these two dates, phytoplankton biomass was very low, 0.6 and 0.5 μg L^{-1}, respectively. The dominant diatom species included *Asterionellopsis glacialis*, *Eucampia zodiacus*, and three species of *Chaetoceros* spp. (*Chaetoceros debilis*, *Chaetoceros contortus*, and *Chaetoceros socialis*), three species of *Thalassiosira* spp. (*T. pacifica/aestivalis*, *T. nordenskioeldii*, and *Thalassiosira rotula*), *Nitzschia* spp., *Navicula* spp., and *Pseudo-nitzschia* spp. Dinoflagellates from the genera of *Protoperidinium* spp., *Alexandrium* spp., and *Gyrodinium* spp. were diverse and abundant in some samples.

In late summer (August–September), phytoplankton biomass had the highest values for the year (Table 1; Fig. 4). The bloom on 27 August of 952.2 μg C L^{-1} was caused by multiple species including dinoflagellates *Prorocentrum gracile* and *Alexandrium* spp., the *Pseudo-nitzschia australis* complex, *T. pacifica/aestivalis*, and *Leptocylindrus danicus*. Low biomass on 10 September (a "post-bloom" date) was followed by a large bloom of *P. gracile* on 22 September (the second highest carbon biomass of 965.2 μg C L^{-1}). A bloom on 5 October (1,907.8 μg C L^{-1}, the highest carbon biomass) again was characterized by a diatom–dinoflagellate mixture. At this time, the dominant diatoms were similar to those in July and August, but with new appearances of *Stephanopyxis palmeriana* and *Lauderia annulata*. Prominent dinoflagellates were *Pyrophacus* sp., *Akashiwo sanguinea*, and *Scrippsiella trochoidea*. On average, dinoflagellates comprised ~68 % of total phytoplankton carbon in comparison with diatoms of 30 %.

In autumn, microscopy results showed that phytoplankton community was composed of dinoflagellates. The peaks of total Chl *a* on 19 October (20.9 μg L^{-1}) and 4 November (20.7 μg L^{-1}) were largely related to a bloom of the dinoflagellate *A. sanguinea*, but there was a high level of Chl *a* in the <5 μm size fraction as well, 64 to 86.2 % of the total Chl *a*. The carbon biomass was 137.5 and 189.5 μg C L^{-1} on the same two dates.

Phytoplankton Community Structure

At the resemblance level of 15 %, three groupings representing seasonal changes in phytoplankton community were separated significantly (CLUSTER result, *p*<0.01). Indeed, the community pattern was distinguished by season (ANOSIM, *R*=0.58, *p*=0.001). CLUSTER groupings were

overlaid on the ordination plot of NMDS (2D stress=0.13; Fig. 5). Group 1 contained "cluster A," which included the winter dates as well as two dates in spring (23 April and 5 May). Biomass was low (Chl *a* <2.2 μg L^{-1}) on each of these dates (Fig. 3; Table 1). Group 2 contained two clusters (B and C). Those dates that clustered as "B" (in the upper part of the circle in Fig. 5) represented the phytoplankton community observed early in the upwelling season when upwelling was strong, primarily from April to July, along with 5 October, a sampling date during the last upwelling event of the year (event "g"; see Fig. 2 or 3). Biomass was relatively high for cluster B, with Chl *a* concentrations ranging from 4 to 14.5 μg L^{-1} (Fig. 6). Cluster "C" dates (in the lower part of the circle in Fig. 5) were from a late upwelling season when upwelling was weak, including cruises on 27 August and 10 and 22 September, with similar values of Chl *a*, as seen for cluster B, 10.3, 3.7, and 15.6 μg L^{-1}, respectively. Group 3 contained cluster D and this was a warm water autumn cluster and contained the dates of 19 October, 4 and 10 November, and 14 June with total Chl *a* of 20.9, 20.7, 2.1, and 0.50 μg L^{-1}, respectively. Thus, even though clusters B, C, and D contained dates with large blooms, each also had dates with low phytoplankton biomass (as measured by Chl *a*).

SIMPER results are shown in Table 2. Cluster A had a total similarity of 25.9. The dominant species in this cluster were the discoid diatoms along with silicoflagellates, *Protoperidinium* spp., and *Gonyaulax* spp. Cluster B (the strong upwelling cluster; SST<~11 °C) clustered more intensively with a total similarity of 42.3. *C. debilis* was the most dominant species due to its individual contribution of 20 %, followed by *Thalassiosira* spp., *A. glacialis*, *Nitzschia* spp., *Pseudo-nitzschia* spp., and *E. zodiacus*. Cluster C (late summer and autumn; SST>11 °C) had a similarity of 33.4. This community was composed of a mixture of dinoflagellates (*P. gracile*, *Protoperidinium* spp., and *A. sanguinea*) and diatoms (*Pseudo-nitzschia* spp., *C. debilis*, and *Thalassiosira* spp.); cluster D showed the second highest similarity (35.3). The dinoflagellate *A. sanguinea* alone contributed 62 % of the total similarity. In summary, clusters A
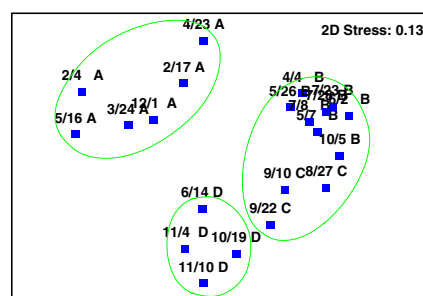

Fig. 5 NMDS plot. Three groupings are symbolized by *three circles*. *A*, *B*, *C*, and *D* are the four clusters
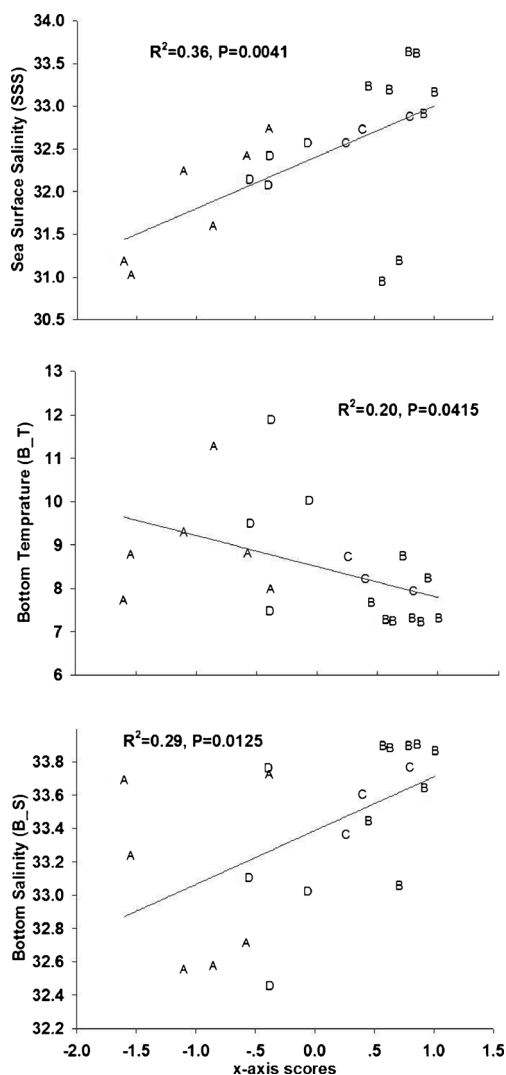
Fig. 6 Relationships between *x*-axis scores derived from NMDS analysis and sea surface salinity (*SSS*), bottom temperature (*B_T*), and bottom salinity (*B_S*). Each sampling date (*points on the plot*) is represented by the *letter* of its corresponding cluster

Table 2 Contributions of taxa to the total similarity of each cluster (A, B, C, and D)

	Av.Bio	Av.Sim	Contrib%	Cum%
Cluster A (cold winter cluster)	Total similarity, 25.9			
Coscinodisoideae	0.6	10.3	39.9	39.9
Silicoflagellates	0.3	6.1	23.6	63.5
Protoperidinium spp.	0.5	4.3	16.4	79.9
Gonyaulax spp.	0.2	2.3	9.0	88.9
Cluster B (strong cold upwelling cluster)	Total similarity, 42.3			
Chaetoceros debilis	4.1	8.3	19.6	19.6
Thalassiosira nordenskioeldii	2.3	3.4	7.9	27.5
Asterionellopsis glacialis	2.8	3.3	7.9	35.4
Thalassiosira rotula	2.6	3.3	7.7	43.1
Nitzschia spp.	1.5	3.1	7.4	50.5
Thalassiosira pacifica/aestivalis	2.4	2.9	6.9	57.3
Pseudo-nitzschia australis complex	1.8	2.9	6.8	64.2
Thalassiosira spp. (<30 μm)	2.2	2.2	5.1	69.3
Chaetoceros contortus	1.3	1.9	4.4	73.7
Coscinodiscaceae	0.8	1.3	3.1	76.8
Navicula spp.	1.1	1.2	2.9	79.6
Eucampia zodiacus	1.5	1.1	2.5	82.2
Cluster C (late upwelling season cluster)	Total similarity, 33.4			
Prorocentrum gracile	4.9	10.4	31.3	31.3
Pseudo-nitzschia australis complex	2.5	5.4	16.2	47.5
Chaetoceros debilis	1.3	4.2	12.7	60.2
Thalassiosira pacifica/aestivalis	2.0	2.4	7.3	67.5
Protoperidinium spp.	1.1	2.3	6.8	74.3
Akashiwo sanguinea	1.8	2.0	6.1	80.4
Cluster D (warm autumn cluster)	Total similarity, 35.3			
Akashiwo sanguinea	3.5	22.0	62.4	62.4
Ceratium lineatum	0.6	4.8	13.7	76.0
Alexandrium catenella	0.5	3.2	9.0	85.0

More important species (80 % of Cum% cutoff) are listed in decreasing order in terms of their respective average similarity (Av.Sim)

Av.Bio average log(*x*+1) transformed carbon biomass (in micrograms C per liter), *Contrib%* similarity contribution of each species to the total cluster, *Cum%* sum of Contrib%

and C were a mixed assemblage of diatoms and dinoflagellates, while cluster B was dominated by diatoms and cluster D was dominated by dinoflagellates.

The Linkage Between Environmental Variables and Phytoplankton Community Structure

Results from the BIO-EVN analysis showed the 10 best combinations (Table 3) of variables. The optimum (highest) $\rho = 0.374$ was found for five variables: NH_4, SST, SSS, bottom temperature (B_T), and bottom salinity (B_S), and was significant at the significance level of 1.1 %. That is to say, the combining factors of temperature, salinity, and ammonium matched well with phytoplankton community structures.

Correlation analysis of *x*-axis scores of the NMDS ordination with oceanographic variables showed the same significant relationships ($p=0.05$; Fig. 6): B_T showed a weakly negative correlation ($R^2=0.20$, $p=0.0415$), while SSS and B_S showed significantly positive correlations ($p=0.0041$ and 0.0125) with phytoplankton species community changes.

There was a significant correlation between Secchi depth and Chl *a* concentration (Fig. 7), suggesting that thick blooms (in excess of 10 μg L^{-1}) became light-limited as Secchi depths approached 3 m depth. This is approximately one third to one fifth the depth of the mixed layer (10–15 m).

Table 3 Best environmental variable combinations with corresponding Spearman's rank correlation coefficients (ρ values) obtained from BIO-EVN analysis

No. of variables in each combination	ρ	Combinations
5	0.374	2, 5, 6, 7, 8
4	0.365	2, 6, 7, 8
4	0.363	5, 6, 7, 8
4	0.359	2, 5, 6, 7
4	0.350	2, 5, 7, 8
3	0.347	2, 6, 7
3	0.347	6, 7, 8
3	0.343	2, 6, 8
3	0.338	5, 6, 7
4	0.334	2, 5, 6, 8

All data are from station NH05

1 PO_4, 2 NH_4, 3 $Si(OH)_4$, 4 NO_3, 5 SST, 6 SSS, 7 temperature at a depth of 50 m, 8 salinity at a depth of 50 m

Discussion

The first half of the year 2009 was anomalously cold due in part to negative values of the Pacific Decadal Oscillation (PDO) throughout the northeast Pacific Ocean. The PDO changed sign in early summer, leading to anomalously warm SST from August onwards. The change in SST at the basin scale caused by variations in basin-scale winds (Mantua et al. 1997) may have been associated with the differences we observed in the strength of the upwelling—upwelling was strong early in the upwelling season during the negative phase of the PDO but then weakened in August, 1 or 2 months earlier than "normal" years, a situation expected during the positive phase of the PDO (Chhak et al. 2009). The phase change of the PDO in summer 2009 may have been related to the development of a weak El Niño event in equatorial waters (Bjorkstedt et al. 2010) at that time.

Chl *a* concentration during our study was highly variable, ranging from 0.4 to 21 µg L^{-1}. Such variability is typical of values seen elsewhere in the coastal upwelling system of the

Fig. 7 Relationship between Secchi depth and Chl *a* concentration

California Current, including off Pt. Reyes (0.9–32.1 µg L^{-1}) (Lassiter et al. 2006) and in Monterey Bay upwelling season (3–15 µg L^{-1}) (Pennington and Chavez 2000). The peak values which we observed were all associated with active upwelling events, except for the October peaks which were associated with a bloom of *A. sanguinea* (Du et al. 2011). On average, the contribution of small cells (those that passed through a 5-µm filter) was >50 % (range, 50–91.6 %) during blooms associated with very high Chl *a* concentrations (9–21 µg L^{-1}) during the upwelling season. These observations differ from the results off northern California (Lassiter et al. 2006) where the highest Chl *a* concentrations were caused mostly by large diatoms instead of nanoflagellates or picoplankton and from coastal waters off Washington State where Chl *a* >5 µm fraction was typically >75 % of total Chl *a*, but similar to the exceptional observation in May–June 2006 off northern Oregon Coast where the median of Chl *a* >5 µm fraction was 43 % (Frame and Lessard 2009). In our study, during moderate winter–spring blooms (<5 µg L^{-1}) and one bloom in July, the >5 µm size fraction accounted for 50–60 % of the total Chl *a*. The two lowest Chl *a* concentrations (below 0.8 µg L^{-1}), however, corresponded to >90 % of Chl *a* in the >5 µm fraction. Thus, during much of the year (especially during the upwelling season), a significant amount of smaller autotrophic components is present in the phytoplankton community throughout the year off central Oregon.

In terms of seasonal variations in species composition, there are, to the best of our knowledge, no published studies on the species or community composition of phytoplankton on a year-round basis from continental shelf waters of the northern California Current off Washington or Oregon. There are two long-term studies in coastal waters on surf-zone diatoms (e.g., Lewin 1978) and harmful algae (Trainer et al. 2002) in the summer off the coast of Washington State but nothing else. Changes in phytoplankton community structure which we observed off Newport followed the Margalef paradigm of diatom dominance in summer and dinoflagellate dominance in autumn (Figueiras et al. 2002; Margalef 1978). Comparable successions from diatoms to dinoflagellates were described by Estrada and Blasco (1979) for the southern California Current, by Mitchell-Innes and Walker (1991), Pitcher et al. (1991), and Fawcett et al. (2007) for the southern Benguela upwelling system, and by Silva et al. (2009) in Lisbon Bay, Portugal. However, at the species level, the dominant diatoms found during the large blooms in our study were not always the same. For example, *C. debilis* and *E. zodiacus* dominated on 8 July, *E. zodiacus* on 23 July, *Thalassiosira* spp. (<30 µm) on 28 July, *Pseudo-nitzschia australis* complex and *P. gracile* on 27 August, and *T. rotula* and *Pyrophacus* sp. on 5 October. Therefore, what we found here is consistent with the conclusions derived by Pitcher et al. (1991) in that changes of phytoplankton species
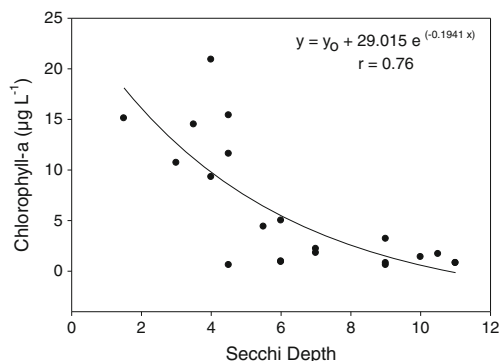
composition in upwelling zones were unpredictable but trends in the dominant patterns of higher taxonomic level, such as diatoms, dinoflagellates, or nanoflagellates, could be discerned.

In our study, we found four community clusters (labeled A through D) that were closely associated with both the seasonal upwelling cycle (winter downwelling, spring/summer upwelling, and autumn downwelling) and within-season upwelling cycle (upwelling and downwelling at the event scale). Concerning the cold "winter" cluster A, when compared to other clusters, nutrient conditions indicate that nitrate was readily available (around 10 μM) but lower than during summer strong upwelling events when values >20 μM were frequently observed. A lack of sufficient light during winter to support photosynthesis is likely the reason for low biological activity and very low phytoplankton biomass at that time. In some years, pronounced winter blooms were seen (e.g., 2002–2005), but in other years (1998–2001), no blooms were seen as described by Feinberg et al. (2010). In 2009, two blooms of moderate scale were observed in winter, on 23 January (2.2 μg L^{-1}) and on 17 February (1.7 μg L^{-1}). We do not know the source of the seed stock for these occasional late winter blooms, and we can only note that there are differences in species composition between the winter blooms ("cold/downwelling" period, as on17 February) and the "cold/upwelling" spring–summer blooms (as on 26 May and 23 and 28 July). Some dominant species appeared in both winter and spring–summer blooms but with dramatic increase in abundance during spring–summer blooms, such as *A. glacialis*, *T. pacifica/aestivalis*, *T. nordenskioeldii*, *Thalassiosira* spp. (<30 μm), *Pseudo-nitzschia* spp., and smaller pennate diatoms. Within the genus of *Chaetoceros*, dominant species exhibited successions from winter to summer: *C. lorenzianus* and *C. teres* were dominant in winter blooms, while *C. debilis*, *Chaetoceros convolutus*, *Chaetoceros affinis*, and *C. socialis* dominant in spring–summer. On the other hand, some species were dominant during spring–summer blooms exclusively, such as *Asterionellopsis socialis*, *Guinardia delicatula*, *E. zodiacus*, and *T. rotula*. As for other taxa, dinoflagellates were more diverse and abundant in spring–summer blooms compared with silicoflagellates and ciliates that had a relatively high abundance during the winter.

Upwelling assemblages in our study were typically dominated by diatoms as seen from cluster B which occurred during sampling dates early in the upwelling season. The dominant genera off central Oregon, as listed previously, were analogous to previous findings at either the species or genus level along the west coast of North America. Horner et al. (2005) reported that the major winter–spring bloom species in Dabob Bay, WA (Puget Sound), included *Skeletonema costatum*, *Thalassiosira* spp., and *Chaetoceros* spp. During summer, the dominant taxa that we observed

were similar to those found along the coasts of northern Oregon and southern Washington during upwelling periods (Frame and Lessard 2009). Off northern California, comparable species were found, including *Chaetoceros* spp., *Thalassiosira* spp., *Asterionellopsis* spp., *S. costatum*, *Nitzschia* spp., and *Rhizosolenia* spp. (Hood et al. 1990; Lassiter et al. 2006). Off southern California, species composition given by Tont (1987) and Venrick (2012) was more or less similar to our observations off Oregon as, for example, *C. debilis*, *Chaetoceros radicans*, and *Pseudo-nitzschia* spp. Beyond the California Current System (CCS), similar phytoplankton species were seen off central Chile (Anabalón et al. 2007), west coasts of Portugal (Silva et al. 2009), Spain (Tilstone et al. 2000), and southern Benguela upwelling water (Pitcher et al. 1991).

The third assemblage, a "late upwelling season" cluster (C) contained a bloom of *P. gracile* on 27 August and 22 September. The cruise on 27 August was subject to an upwelling event (event "f" in Fig. 2) and was associated with nutrient peaks and lower SST than dates before or after this cruise. The decline of diatoms was seen on 10 September associated with low nutrient concentrations and onshore transport of warm water and was followed by a monospecific bloom of *P. gracile* on 22 September. The fourth assemblage (cluster D) was in the "warm autumn" period and was defined by a bloom of *A. sanguinea* from October to November, previously described by Du et al. (2011). The physical conditions associated with these dinoflagellate blooms are within the broad range described for most dinoflagellate blooms in upwelling systems (Kudela et al. 2010; Smayda and Trainer 2010) in that they occurred late in the upwelling season.

Correlations among commonly used measures of phytoplankton biomass such as total Chl a and Chl a >5 μm concentrations and environmental variables were not significant. This indicates that phytoplankton biomass could not be predicted exclusively by the available environmental factors. The BEST/BIO-EVN analysis indicated that ammonium, temperature, and salinity together were important in shaping phytoplankton community patterns, whereas macronutrients (NO_3, PO_4, and $Si(OH)_4$) did not appear as significant factors. Correlations with temperature and salinity are likely related to offshore–onshore advection associated with the alternation of active relaxation of the upwelling process. Lack of correlation with macronutrients (e.g., nitrate) arose because we found that high nitrate concentrations can be associated with both low and high phytoplankton biomass: nitrate was high but phytoplankton biomass was low in samples collected early in upwelling events ($n=4$) and nitrate was high while phytoplankton biomass was moderately high in samples collected during upwelling events ($n=3$).

Large blooms were seen *only near the end* of upwelling events as the winds began to relax, a common observation

(Barber and Smith 1981; Estrada and Blasco 1979; Mitchell-Innes and Walker 1991; Small and Menzies 1981). The formation of large diatom blooms in upwelling systems often requires a 3- to 7-day "relaxation window"—at such times, the water column stratifies, allowing the rapid growth of cells. Wetz (2003) incubated freshly upwelled water collected off Newport, OR in 20-L cubitainers during August 2001 and found that the maxima in chlorophyll occurred 5 days after incubation was initiated and that all nutrients were consumed by the fourth day. He carried out two experiments in early August and two in late August. The first two experiments were dominated by *Chaetoceros* spp.; during the latter two experiments, *Chaetoceros* spp. dominated in one cubitainer and *Leptocylindrus minimus* in the second. Similarly, Wilkerson and Dugdale (1987), working in the southern California Current, filled large (380 L) barrels with freshly upwelled seawater aboard ship and tracked changes in nutrients and chlorophyll, with the result that blooms appeared within 4 days. Tilstone et al. (2000) provide an example from the upwelling system off Portugal whereby the *Thalassiosira* spp. and *S. costatum* assemblage was affected by the hydrographic process more than the biogeochemical process, resulting in a net loss of these cells by being exported away from shore during a persistent period of upwelling, in contrast with the assemblage of *Chaetoceros* spp. and *Cerataulina pelagica*, which maintained a high standing stock due to their higher growth rates during upwelling period and continued to accumulate cells during upwelling relaxation.

Mitchell-Innes and Walker (1991) suggested that phytoplankton blooms in the coastal upwelling zone of the southern Benguela Current were controlled by multiple factors including nutrient sources in upwelled water, vertical mixing, and regenerated nutrients (ammonium and urea) in the upper water column. Though ammonium concentrations were low in our study (0.02–1.43 μM), both high and low phytoplankton biomass and Chl *a* concentration were related with an even lower range (0–0.04 μM). Probyn (1985) noted that nitrate was quantitatively the largest portion of total nitrogen and 71 % of total was assimilated on the shelf in Benguela upwelling system, but picoplankton, nanoplankton, and the community of larger phytoplankton species showed a consistent preference for ammonium. The size-fractionated chlorophyll composition off central Oregon Coast displayed a high and constant proportion of Chl *a* <5 μm fraction. Ammonium consumption might be related with the high concentration of smaller cells. In waters off Newport, OR, Dickson and Wheeler (1995) reported that ammonium uptake rates were the highest during the upwelling season and the lowest during the non-upwelling season. They also found that phytoplankton uptake rates on nitrate were saturated when its concentrations were >5 μM. Dugdale et al. (2007) concluded that a critical range of ammonium concentration from 1 to 4 μM

caused low nitrate uptake, but this kind of inhibition process was not likely to occur in the present study because ammonium concentrations were low throughout the year. Wilkerson et al. (2006) observed ammonium consumption by smaller-sized phytoplankton during post-upwelling and autumn blooms in San Francisco Bay. Kudela et al. (2010) suggested high concentrations of regenerated nitrogen (ammonium and urea) were able to sustain flagellates as well as diatom *Pseudo-nitzschia* spp. blooms in upwelling systems. Taken together, the significant concentration of smaller cells, the potentially flexible consumption on ammonium by most phytoplankton size fractions, and the versatile physical conditions led to a closer correlation between ammonium and phytoplankton assemblages than other nitrogen forms.

Summary and Conclusions

A pronounced seasonal cycle in the species composition and biomass of phytoplankton was observed throughout the year. Of the larger phytoplankton cells, four community types were identified: a mixed-taxa low-biomass community in winter, a diatom-type high-biomass community during spring/summer, a mixed-taxa high-biomass community in late summer, and a dinoflagellate-dominated high-biomass community in autumn. Several large diatom blooms from April to August and a very large bloom in October/November due to *A. sanguinea* sequentially occurred. The community composition changes showed significant correlations with B_T, B_S, and SSS. We did not find significant correlations between phytoplankton biomass and environmental variables which should not be surprising because our sampling at fortnightly intervals could not be expected to resolve the dynamics of phytoplankton growth—this can only be resolved by daily sampling over long periods of time. This is rarely accomplished (a notable exception being a daily time series of sampling, for 27 days, by Mitchell-Innes and Walker 1991 in the southern Benguela upwelling system).

Missing from our study was the consideration of sources of the seed stock for blooms, a topic investigated by Smith et al. (1983) for the upwelling system off Peru and recently reviewed by Smayda and Trainer (2010). Are blooms seeded locally from spores on the sea floor or are blooms seeded by advection with different water masses into our study region? To date, little information has been published on advection of phytoplankton species with seasonal currents in the CCS. Venrick (2009) examined the idea of advection of species to southern California from the north by the California Current, but she found no unique flora—the phytoplankton species in the southern assemblages were analogous to the north. On the other hand, Hill and Wheeler (2002) found that much higher levels of particulate carbon and nitrogen were brought in the CCS from subarctic or transition waters than from

subtropical gyres. Similarly, Du et al. (2011) suggested that the bloom of *A. sanguinea* found off Oregon in 2009 was transported from the north (along coastal waters off Washington State).

References

Anabalón, V., C.E. Morales, R. Escribano, and M. Angélica Varas. 2007. The contribution of nano- and micro-planktonic assemblages in the surface layer (0–30 m) under different hydrographic conditions in the upwelling area off Concepción, central Chile. *Progress in Oceanography* 75: 396–414.

Auth, T.D. 2011. Analysis of spring–fall epipelagic ichthyoplankton community in the northern California Current in 2004–2009 and its relation to environmental factors. *CalCOFI Report* 52: 148–167.

Barber R. T., and R. L. Smith. 1981. Coastal upwelling ecosystems. In *Analysis of marine ecosystems*, ed. A. R. Longhurst, 31–68. London: Academic.

Bjorkstedt, E.P., R. Goericke, S. McClatchie, E. Weber, W. Watson, N. Lo, W. Peterson, B. Emmett, J. Peterson, R. Durazo, G. Gaxiola-Castro, F. Chavez, J.T. Pennington, C.A. Collins, J. Field, S. Ralston, K. Sakuma, S. Bograd, F. Schwing, Y. Xue, W. Sydeman, S.A. Thompson, J.A. Santora, J. Largier, C. Halle, S. Morgan, S.Y. Kim, K. Merkens, J. Hildebrand, and L. Munger. 2010. State of the California Current 2009–2010: Regional variation persists through transition from La Niña to El Niño (and back?). *California Cooperative of Oceanographic Fisheries Investigations Reports* 51: 39–69.

Chavez, F.P., R.T. Barber, P.M. Kosro, A. Huyer, S.R. Ramp, T.P. Stanton, and B. Rojas de Mendiola. 1991. Horizontal transport and the distribution of nutrients in the coastal transition zone off northern California: Effects on primary production, phytoplankton biomass and species composition. *Journal of Geophysical Research* 96: 14833–14848.

Chhak, K.C., E. Di Lorenzo, N. Schneider, and P.F. Cummins. 2009. Forcing of low-frequency ocean variability in the northeast Pacific. *Journal of Climate* 22: 1255–1276.

Clarke, K.R., and R.N. Gorley. 2006. *PRIMER v6: User manual/tutorial*. Plymouth: PRIMER-E Ltd.

Dickson, M.L., and P.A. Wheeler. 1995. Nitrate uptake rates in a coastal upwelling regime—A comparison of PN-specific, absolute, and Chl *a*-specific rates. *Limnology and Oceanography* 40: 533–543.

Du, X., W. Peterson, A. McCulloch, and G. Liu. 2011. An unusual bloom of the dinoflagellate *Akashiwo sanguinea* off the central Oregon, USA, coast in autumn 2009. *Harmful Algae* 10: 784–793.

Dugdale, R.C., F.P. Wilkerson, V.E. Hogue, and A. Marchi. 2007. The role of ammonium and nitrate in spring bloom development in San Francisco Bay. *Estuarine, Coastal and Shelf Science* 73: 17–29.

Estrada, M., and D. Blasco. 1979. Two phases of the phytoplankton community in the Baja California upwelling. *Limnology and Oceanography* 24: 1065–1080.

Fawcett, A., G.C. Pitcher, S. Bernard, A.D. Cembella, and R.M. Kudela. 2007. Contrasting wind patterns and toxigenic phytoplankton in the southern Benguela upwelling system. *Marine Ecology Progress Series* 348: 19–31.

Feinberg, L.R., and W.T. Peterson. 2003. Variability in duration and intensity of euphausiid spawning off central Oregon, 1996–2001. *Progress in Oceanography* 57: 363–379.

Feinberg, L.R., W.T. Peterson, and T.C. Shaw. 2010. The timing and location of spawning for the Euphausiid *Thysanoessa spinifera* off the Oregon Coast, USA. *Deep-Sea Research II* 57: 572–583.

Figueiras, F.G., U. Labarta, and M.J. Fernández Reiriz. 2002. Coastal upwelling, primary production and mussel growth in the Rías Baixas of Galicia. *Hydrobiologia* 484: 121–131.

Frame, E.R., and E.J. Lessard. 2009. Does the Columbia River plume influence phytoplankton community structure along the Washington and Oregon coasts? *Journal of Geophysical Research* 114: C00B09. doi:10.1029/2008JC004999.

Henson, S.A., and A.C. Thomas. 2007. Interannual variability in timing of bloom initiation in the California Current system. *Journal of Geophysical Research* 112: C08007.

Hickey, B.M. 1989. Patterns and processes of circulation over the shelf and slope. In *Coastal oceanography of Washington and Oregon*, ed. M.R. Landry and B.M. Hickey, 41–116. Amsterdam: Elsevier.

Hickey, B.M., and N.S. Banas. 2008. Why is the northern end of the California Current system is so productive? *Oceanography* 21: 90–107.

Hill, J.K., and P.A. Wheeler. 2002. Organic carbon and nitrogen in the northern California Current system: Comparison of offshore, river plume, and coastally upwelled waters. *Progress in Oceanography* 53: 369–387.

Hood, R.R., M.R. Abbott, A. Huyer, and P.M. Kosro. 1990. Surface patterns in temperature, flow, phytoplankton biomass, and species composition in the coastal transition zone of northern California. *Journal of Geophysical Research* 95: 18081–18094.

Hooff, R.C., and W.T. Peterson. 2006. Recent increases in copepod biodiversity as an indicator of changes in ocean and climate conditions of the northern California Current ecosystem. *Limnology and Oceanography* 51: 2607–2620.

Horner, R.A. 2002. *A taxonomic guide to some common phytoplankton*. Bristol: Biopress Ltd.

Horner, R.A., J.R. Postel, C. Halsband-Lenk, J.J. Pierson, G. Pohnert, and T. Wichard. 2005. Winter–spring phytoplankton blooms in Dabob Bay, Washington. *Progress in Oceanography* 67: 286–313.

Huyer, A. 1977. Seasonal variation in temperature, salinity and density over the continental shelf off Oregon. *Limnology and Oceanography* 22: 442–453.

Kudela, R.M., J.P. Ryan, M.D. Blakely, J.Q. Lane, and T.D. Peterson. 2008. Linking the physiology and ecology of *Cochlodinium* to better understand harmful algal bloom events: A comparative approach. *Harmful Algae* 7: 278–292.

Kudela, R.M., S. Seeyave, and W.P. Cochlan. 2010. The role of nutrients in regulation and promotion of harmful algal blooms in upwelling systems. *Progress in Oceanography* 85: 122–135.

Lassiter, A.M., F.P. Wilkerson, R.C. Dugdale, and V.E. Hogue. 2006. Phytoplankton assemblages in the CoOP-WEST coastal upwelling area. *Deep-Sea Research II* 53: 3063–3077.

Lewin J. 1978. Blooms of surf-zone diatoms along the coast of the Olympic Peninsula, Washington: IX. Factors controlling the seasonal cycle of nitrate in the surf at Copalis Beach (1971–1985). *Estuarine and Coastal Marine Science* 7: 173–183.

Mantua, N.J., S.R. Hare, Y. Zhang, J.M. Wallace, and R.C. Francis. 1997. A Pacific interdecadal climate oscillation with impacts on salmon production. *Bulletin in the American Meteriological Society* 78: 1069–1079.

Margalef, R. 1978. Life-forms of phytoplankton as survival alternatives in an unstable environment. *Oceanologica Acta* 134: 493–509.

Menden-Deuer, S., and E.J. Lessard. 2000. Carbon to volume relationships for dinoflagellates, diatoms and for other protist plankton. *Limnology and Oceanography* 45: 569–579.

Menden-Deuer, S., E.J. Lessard, and J. Stterberg. 2001. Effects of preservation on dinoflagellate and diatom cell volume and consequences for carbon biomass predictions. *Marine Ecology Progress Series* 222: 41–50.

Mitchell-Innes, B.A., and D.R. Walker. 1991. Short-term variability during an anchor station study in the southern Benguela upwelling system: Phytoplankton production and biomass in relation to specie changes. *Progress in Oceanography* 28: 65–89.

Newton, J.A., and R.A. Horner. 2003. Use of phytoplankton species indicators to track the origin of phytoplankton blooms in Willapa Bay, Washington. *Estuaries* 26: 1071–1078.

Olson, M.B., and E.J. Lessard. 2008. The influence of the *Pseudo-nitzschia* toxin, domoic acid, on microzooplankton grazing and growth: A field and laboratory assessment. *Harmful Algae* 9: 540–547.

Pennington, J.T., and F.P. Chavez. 2000. Seasonal fluctuations of temperature, salinity, nitrate, chlorophyll and primary production at a station H3/M1over 1989–1996 in Monterey Bay, California. *Deep-Sea Research II* 47: 947–973.

Peterson, W.T., and J.E. Keister. 2003. Interannual variability in copepod community composition at a coastal station in the northern California Current: A multivariate approach. *Deep-Sea Research II* 50: 2499–2517.

Peterson, W.T., and C.B. Miller. 1977. Seasonal cycle of zooplankton abundance and species composition along the central Oregon Coast. *Fishery Bulletin US* 75: 717–724.

Peterson, W.T., J. Gómez-Gutiérrez, and C.A. Morgan. 2002. Cross-shelf variation in calanoid copepod production during summer 1996 off the Oregon Coast, USA. *Marine Biology* 141: 353–365.

Pitcher, G.C., D.R. Walker, B.A. Mitchell-Innes, and C.L. Moloney. 1991. Short-term variability during an anchor station study in the southern Benguela upwelling system: Phytoplankton dynamics. *Progress in Oceanography* 28: 39–64.

Pitcher, G.C., F.G. Figueiras, B.M. Hickey, and M.T. Moita. 2010. The physical oceanography of upwelling systems and the development of harmful algal blooms. *Progress in Oceanography* 85: 5–32.

Probyn, T.A. 1985. Nitrogen uptake by size-fractioned phytoplankton populations in the southern Benguela upwelling system. *Marine Ecology Progress Series* 22: 249–258.

Silva, A., S. Palma, P.B. Oliveira, and M.T. Moita. 2009. Composition and interannual variability of phytoplankton in a coastal upwelling region (Lisbon Bay, Portugal). *Journal of Sea Research* 62: 238–249.

Small, L.F., and D.W. Menzies. 1981. Patterns of primary production in a coastal upwelling region. *Deep Sea Research Part A* 28: 123–149.

Smayda, T.J., and V.L. Trainer. 2010. Dinoflagellate blooms in upwelling systems: Seeding, variability, and contrasts with diatom bloom behaviour. *Progress in Oceanography* 85: 92–107.

Smith, W.O., G.W. Heburn, R.T. Barber, and J.J. O'Brien. 1983. Regulation of phytoplankton communities by physical processes in upwelling ecosystems. *Journal of Marine Research* 41: 539–556.

Strickland, J.D.H., and T.R. Parsons. 1972. *A practical handbook of sea-water analysis (2nd ed)*. Ottawa: Fisheries Research Board of Canada.

Thomas, A.C., P. Brickley, and R. Weatherbee. 2009. Interannual variability in chlorophyll concentrations in the Humboldt and California Current systems. *Progress in Oceanography* 83: 386–392.

Tilstone, G.H., B. Martin Miguez, F.G. Figueiras, and E.G. Fermin. 2000. Diatom dynamics in a coastal ecosystem affected by upwelling: Coupling between species succession, circulation and biogeochemical processes. *Marine Ecology Progress Series* 205: 23–41.

Tont, S.A. 1987. Variability of diatom species populations: From days to years. *Journal of Marine Research* 45: 985–1006.

Trainer, V.L., B.M. Hickey, and R.A. Horner. 2002. Biological and physical dynamics of domoid acid production off the Washington coast. *Limnology and Oceanography* 47: 1438–1446.

Tweddle, J.F., P.G. Strutton, D.G. Foley, X.L. Higgins, A.M. Wood, B. Scott, R.C. Everroad, W.T. Peterson, D. Cannon, M. Hunter, and Z. Forster. 2010. Relationships among upwelling, phytoplankton blooms, and phycotoxins in coastal Oregon shellfish. *Marine Ecology Progress Series* 405: 131–145.

Venrick, E.L. 2009. Floral patterns in the California Current: The coastal-offshore boundary zone. *Journal of Marine Research* 67: 89–111.

Venrick, E.L. 2012. Phytoplankton in the California Current system off southern California: Changes in a changing environment. *Progress in Oceanography* 104: 46–58.

Wetz M. S. 2003. Production and partitioning of organic matter during simulated phytoplankton blooms. M.S. thesis, Oregon State University, 92 p.

Wilkerson, F.P., and R.C. Dugdale. 1987. The use of large shipboard barrels and drifters to study the effects of coastal upwelling on phytoplankton dynamics. *Limnology and Oceanography* 32: 368–382.

Wilkerson, F.P., R.C. Dugdale, V.E. Hogue, and M. Albert. 2006. Phytoplankton blooms and nitrogen productivity in San Francisco Bay. *Estuaries and Coasts* 29: 401–416.

Yoo, S.-J., H.P. Batchelder, W.T. Peterson, and W.J. Sydemann. 2008. Seasonal, interannual and event scale variation in North Pacific ecosystems. *Progress in Oceanography* 77: 155–181.